Journal of Cardiovascular Computed Tomography 13 (2019) 305–314

Contents lists available at ScienceDirect

Journal of Cardiovascular Computed Tomography

journal homepage: www.elsevier.com/locate/jcct

Research paper

Non obstructive high-risk plaque but not calcified by coronary CTA, and the G-score predict ischemia

Gudrun M. Feuchtner[a,*], Fabian Barbieri[b], Christian Langer[a], Christoph Beyer[a], Gerlig Widmann[a], Guy J. Friedrich[b], Fabiola Cartes-Zumelzu[a], Fabian Plank[b]

[a] Dept. Radiology, Innsbruck Medical University, Austria
[b] Dept. Internal Medicine III, Cardiology, Innsbruck Medical University, Austria

ABSTRACT

Background: The association of plaque morphology with ischemia in non-obstructive lesions has not been fully eludicated: Calcium density and high-risk plaque features have not been explored.

Objectives: to assess whether high-risk plaque or calcified, and global mixed including non-calcified plaque burden (G-score) by coronary CTA predict ischemia in non-obstructive lesions using non-invasive fractional flow reserve (FFR_{CT}).

Methods: In 106 patients with low-to-intermediate pre-test probability referred to coronary 128-slice dual source CTA, lesion-based and distal FFR_{CT} were computated.

The 4 high-risk-plaque criteria: Low-attenuation-plaque, Napkin Ring Sign, positive remodelling and spotty calcification were recorded. Plaque density (HU) and stenosis (MLA,MLD,%area,%diameter stenosis) were quantified. Plaque composition was classified as type 1–4:1 = calcified, 2 = mixed (calcified > non-calcified), 3 = mixed (non-calcified > calcified), 4 = non-calcified, and expressed by the **G-score**: Z = Sum of type 1–4 per segment. The total plaque segment involvement score (SIS) and the Coronary Calcium Score (Agatston) were calculated.

Results: 89 non–obstructive lesions were included. Both lesion-based and distal FFR_{CT} were lower in high-risk-plaque as compared to calcified (0.85 vs 0.93, $p < 0.001$ and 0.79 vs 0.86, $p = 0.002$). The prevalence of lesion-based ischemia ($FFR_{CT} < 0.8$) was higher in high-risk-plaque as compared to calcified (25% vs. 2.5%, $p = 0.007$). Similarly, the rate of distal ischemia (40% vs 17.5%) was higher, respectively.

Lower plaque density (HU) indicating higher lipid plaque component ($p = 0.024$) predicted lesion based FFR_{CT} in low attenuation plaque. For all lesions ($n = 89$) including calcified ($p = 0.003$), the correlation enhanced.

Positive remodelling and an increasing non-calcified plaque burden (G-score) in relation to calcified were associated with lower FFR_{CT} distal ($p = 0.042$), but not the SIS and calcium score.

Conclusion: High-risk-plaque but not calcified, an increasing lipid-necrotic-core component and non-calcified mixed plaque burden (G-score) predict ischemia in non-obstructive lesions (INOCA), while an increasing calcium compactness acts contrary.

1. Introduction

Coronary computed tomography angiography (CTA)[1,2] is a non-invasive imaging modality for the evaluation of patients with low-to-intermediate pre-test probability of coronary artery disease (CAD).[1–3] 3D dynamic computational fluid modelling (CFD)[4–8] allows for calculation of the fractional flow reserve[9,10] from CTA (FFR_{CT}). Noninvasive FFR_{CT} from CTA improves accuracy of coronary CTA[5–8] to 93% sensitivity and 82% specificity for detection of lesion-based ischemia, and is efficient for patient management and in order to reduce downstream testing costs.[7]

The advantage of CTA lies in its ability for atherosclerotic plaque characterization[11]: The differentiation of fibroatheroma low attenuation plaque from calcified lesions based on Hounsfield Units (HU), and the identification of high-risk plaque (HRP) predicting major adverse cardiac events (MACE),[12–17] is feasible. Four major HRP-criteria have been inaugurated: Low attenuation plaque (LAP), Napkin Ring Sign (NRS),[12] remodelling index (RI) > 1.1 and spotty calcification < 3 mm, indicate advanced complex atherosclerotic lesions.

Atypical chest pain is the most common complaint in patients referred to coronary CTA, but the morphological correlate (cardiac vs non-cardiac origine) remains often unclear. Especially atypical chest pain could be caused by **ischemia despite non-obstructive coronary artery stenosis (INOCA)**. However studies exploring which plaque types determined by coronary CTA are the main triggers, are sparse. Previous studies included mainly obstructive lesions (prevalence ≈80%),[18] or enrolled small sample size cohorts.

Therefore, the purpose of our study was 1) to compare high risk

* Corresponding author. Dept. Radiology, Innsbruck Medical University, Anichstr. 35, A-6020, Innsbruck, Austria.
E-mail address: Gudrun.Feuchtner@i-med.ac.at (G.M. Feuchtner).

https://doi.org/10.1016/j.jcct.2019.01.010
Received 24 September 2018; Received in revised form 11 November 2018; Accepted 3 January 2019
Available online 04 January 2019
1934-5925/

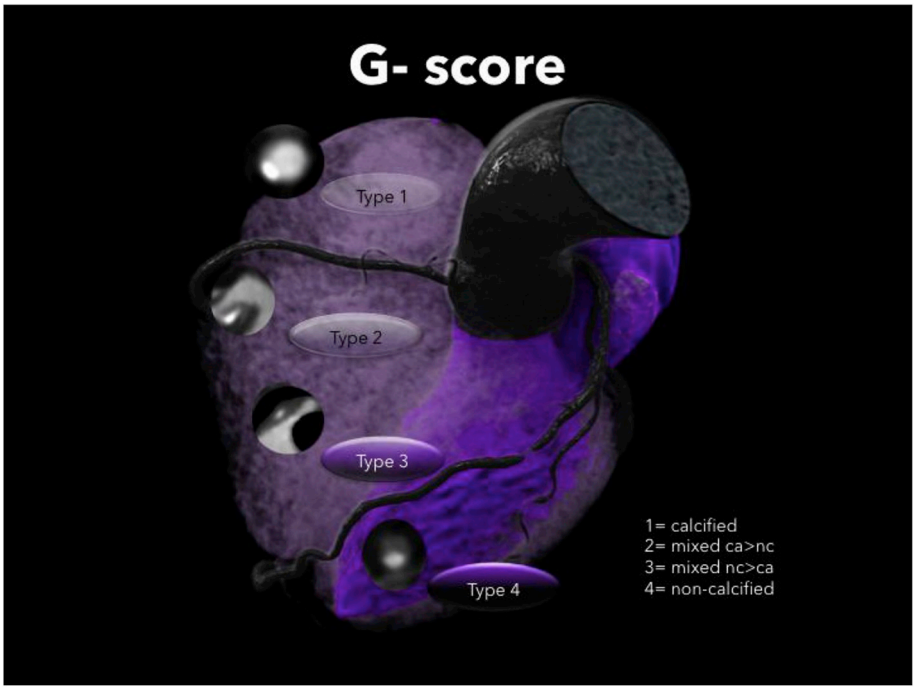

Fig. 1. G-score: Sum of plaque types[1–4] per coronary segment (AHA-16-segment classification).[21]

plaque quantified by coronary CTA with calcified for prediction of lesion based FFR_{CT} and distal FFR_{CT} in non-obstructive lesions, in a low-to-intermediate pre-test probability cohort referred to CTA.

2) to assess whether total, calcified, and an increasing non-calcified plaque burden, as expressed by a novel visual score, the **G-score,** predicts distal ischemia.

2. Methods

2.1. Study design and population

This prospective cohort study was approved by our local institutional review board (IRB). Consecutive patients with intermediate pre-test probability[19] referred to coronary CTA for clinical indications[20] were recruited between 2015 and 2017 into our database. 136 patients were retrospectively selected and sent to FFR_{CT} analysis. Datasets of 106 patients with optimal CTA image quality were finally included into this study.

Inclusion criteria were:

- Nonobstructive lesions with < 70% stenosis. (CAD RADS 0–3)[20]
- low-to-intermediate pre-test probability of CAD (atypical or typical chest pain, or non-specific symptoms with suspected CAD based on treadmill ECG-stress test) according to updated Diamond Forrester[19]

Exclusion criteria were:

- previous percutaneous coronary intervention (PCI)
- previous coronary artery bypass grafting (CABG)
- renal dysfunction (GFR < 45 ml/min/1.73 m^2)
- pregnancy
- age < 21years.
- obstructive lesions > 70%
- tandem lesions (if one of those > 50%)

Conventional coronary risk factors according to standardized European Society Cardiology (ESC) criteria were collected: arterial hypertension (systolic blood pressure > 140 mmHg or diastolic > 90 mmHg), dyslipidemia (cholesterol > 200 mmol/dl or HDL < 40 mmol/l), positive family history (Myocardial infarct (MI) or sudden cardiac death in an immediate male relative < 55y or female < 65y), smoker (current or quit within last 6 months) and diabetes.

Symptoms were recorded prior to CT and stratified as 0 = "non-specific CP or dyspnoe and/or suspected CAD by treadmill ECG-stress test 1 = atypical angina CP or 2 = typical angina stable CP, or 3 = non-specific chest pain or symtoms (eg. 1x acute chest pain).

2.2. Non-contrast CT

Non-contrast ECG-gated coronary calcium score (CCS) with standardized scan parameters (detector collimation 64 × 1.5 mm; 120 kV) was performed. The Agatston Score was calculated.

2.3. Computed tomography angiography (CTA)

Coronary CTA was performed with a 128-slice dual source CTA (*Definition FLASH, Siemens)* (until 06/2011) with a detector collimation of 2 × 64 × 0.6 mm and a z-flying spot and a rotation time 0.28s respectively. Prospective ECG-triggering was used in regular heart rates < 65bpm (diastolic padding, 70% of RR-interval) and in heart rates > 65bpm and irregular rates, retrospective ECG-gating was applied.

An iodine contrast agent (*Iopromide, Ultravist 370™)* was injected intravenously (flow rate 4–6 ml/s + 40 cc saline chaser), triggered into arterial phase (bolus tracking; 100HU threshold; ascending aorta). The contrast volume (65–110 cc) was adjusted according to the patients body weight and scan time using standardized recommendations. Axial images were reconstructed with 0.75 mm slice width (increment 0.4/medium-smooth kernel B26f) during best diastolic and systolic phase.

CTA image analysis. Curved *multiplanar reformations (cMPR)* and oblique interactive MPR of all vessels using 3-D postprocessing software (*SyngoVia™, Siemens*) were generated:

1) **Coronary stenosis severity** was scored visually as: minimal < 25%, mild ≤ 25–49%; intermediate 50–69% or severe ≥70%

Table 1
Study population (n = 106).

age (y)	56.1 ± 12 (range, 26–83)
males (%)	75 (70.7%)
body mass index (kg/m^2)	25.3 ± 3.1 (range, 18.4–36.7)
risk factors	
arterial hypertension	38 (35.8%)
nicotine	20 (18.9%)
positive family history	40 (37.7%)
dyslipidemia	41 (38.7%)
diabetes	4 (3.7%)
symptoms	
Atypical CP	82 (79.2%)
typical stable CP	17 (16.04%)
other *	5 (4.7%)

Table 2
Lesions characteristics (CADRADS- stenosis; plaque type; AHA segments).

Stenosis severity	CADRADS	N (%)
minimal < 25%	1	55 (61.8%)
mild < 50%	2	25 (28.1%)
intermediate 50–70%	3	9 (10.1%)
	Plaque type	N (%)
calcified	1	40 (44.9%)
Mixed Ca > nc	2	14 (15.7%)
Mixed nc > Ca	3	12 (13.5%)
nc	4	23 (25.8%)
AHA segment		
LM		8 (9.9%)
LAD S6		38 (42.7%)
LAD S7		18 (20.2%)
CX S11		6 (6.7%)
RCA S1		9 (10.1%)
RCA S2		7 (7.9%)
RCA S3		2 (2.2%)
DG 1		1 (1.1%)

Abb.: nc = non-calcified, Ca = calcified, LM = left main, LAD = left anterior descending, CX = circumflex artery, RCA = right coronary artery, DG = diagonal branch.

Table 3a
High–Risk Plaque (HRP) versus calcified: distal and lesion FFR_{CT}.

	HRP N = 40	Calcified N = 40	p-value
lesion FFR_{CT}	0.85 ± 10.3	0.93 ± 4.04	p < 0.001*
lesion FFR_{CT} < 0.80	10 (25%)	1 (2.5%)	p = 0.007**
distal FFR_{CT}	0.79 ± 11.7	0.86 ± 5.6	p = 0.002*
distal FFR_{CT} < 0.80	16 (40%)	7 (17.5%)	p = 0.048***

according to CADRADS[20] per-coronary segment (AHA-modified-16-segment classification).[21]

2) **Plaque types** were characterized as: calcified (T1), mixed (dominantly calcified > non-calcified) (T2), mixed (dominantly non-calcified > calcified) (T3), noncalcified (T4) per coronary segment[21] as previously described.[22] Calcified and non-calcified plaque were defined as hyper- and hypoattenuating lesions.[23]

respectively. The coronary segment involvement score (SIS) score[11] was calculated, and the G-score (=Sum of Plaque types T1-4 for each segment) (Fig. 1), as marker for an increasing non-calcifying vs calcified plaque burden, per-coronary segment (AHA-modified-16-segment classification).[21]

3) Quantitative High-risk plaque (HRP)-analysis
- Low attenuation plaque (LAP) = hypodense compared to vessel lumen. CT-density was screened by utilizing "pixel-lens" and the minimal HU was recorded. Then, an area-ROI was placed into the lowest density plaque area, and drawn as large as possible, while sparing areas affected by artifacts from motion, streaks or beam-hardening/partial volume artifacts adjacent to calcifications.
- Napkin Ring Sign was defined[12] as an outer high-density rim (< 200HU) with an inner hypodense area (< 130 HU), which was 1) not adjacent to a calcification (to avoid beam hardening artifact) and 2) present on a minimum of 2 adjacent axial 1 mm slices[16]
- Spotty calcification, defined as calcification < 3 mm size.
- The remodelling index (RI) was calculated as the ratio of the maximal cross-sectional vessel diameter including the plaque and the lumen, and its closest proximal (or distal: in ostial lesions) normal reference vessel lumen diameter. A RI > 1.1 was defined as "positive remodelling".

  If a patient had multiple lesions, all lesions were quantified separately.

A "HRP" was defined, if 2 of 4 criteria were present.[20] For LAP < 60HU cutoff was set as "HRP" group criterion.[16] In mixed T2-lesions, LAP component was only quantified if deemed large enough and not affected by adjacent artifacts.

If the lesion contained a calcified component (T1, T2, T3), a ROI was placed into the calcium on a cross sectional orthogonal image (drawn as large as possible) and the mean HU were recorded).

4) **Quantitative CTA (qCTA)** vessel lumen and stenosis **of the target lesion** (minimal lumen area (MLA), minimal lumen diameter (MLD), % area and % diameterstenosis) were measured with dedicated software (SyngoVIA, Siemens) on curved multiplanar reformations (cMPR) along a centerline. Manual adjustments were made if deemed necessary in case of inaccurate outer contour tracing. If there was a mismatch between 1) visual scoreing and 4) qCTA, the CADRADS lesion was reclassified according to qCTA.

CTA Image analysis was performed by 1 master observer (> 10 years experience, level III SCCT) and a 2nd independent observer with > 6 month training (level II SCCT) independently. Consensus reading was obtained.

Fractional flow reserve by CT (FFR_{CT}) analysis. Axial source CTA images were transferred as DICOM via a Server to a dedicated 3 D-computational fluid dynamic modelling (CFD) software (Heartflow Inc., California, USA). The FFR_{CT} was calculated for all vessels > 1.8 mm. Patients were prepared according to standardized recommendations.[4–7]

Primary endpoint: *Lesion based FFR_{CT}*, measured 2 cm after the maximum lumen narrowing (% stenosis) on CTA. (head-to-head matching) The 3D FFR_{CT} models were interactively rotated, and the lesion was determined head-to-head with the CTA image.

Secondary endpoint. Distal vessel FFR_{CT} was identified for each main vessel and side branch."Ischemia" was defined as FFR_{CT} < 0.8.[10]

2.4. Statistical analysis

Quantitative variables are expressed as means ± standard deviation (SD), categorical variables reported as absolute values and percentages. Normal distribution was tested with Kolomogorow' test and Histogramm.

Mean differences between parametric data were tested by using the independent *t*-test or Mann–Whitney U according to their distribution (*t*-test for normally, and Mann Whitney U for non-normally distributed and rank-scale data).

Differences in categorial data (prevalence of FFR_{CT} < 0.8 in HRP vs Ca) were determined with Chi-Square or Fisher's exact test (if n= < 5

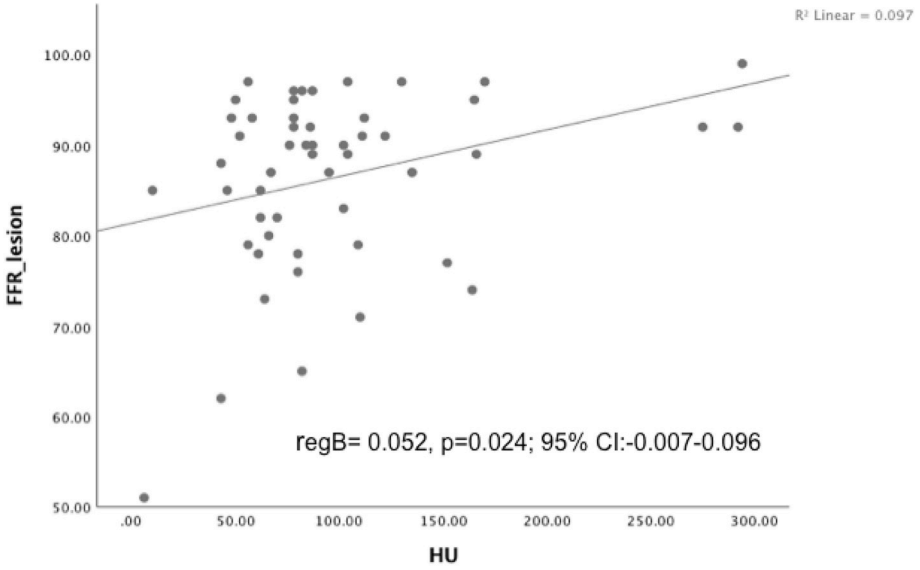

Fig. 2a. The association of low attenuation plaque density (HU) with lower lesion based FFR_{CT} (n = 52, lesions < 300 HU).

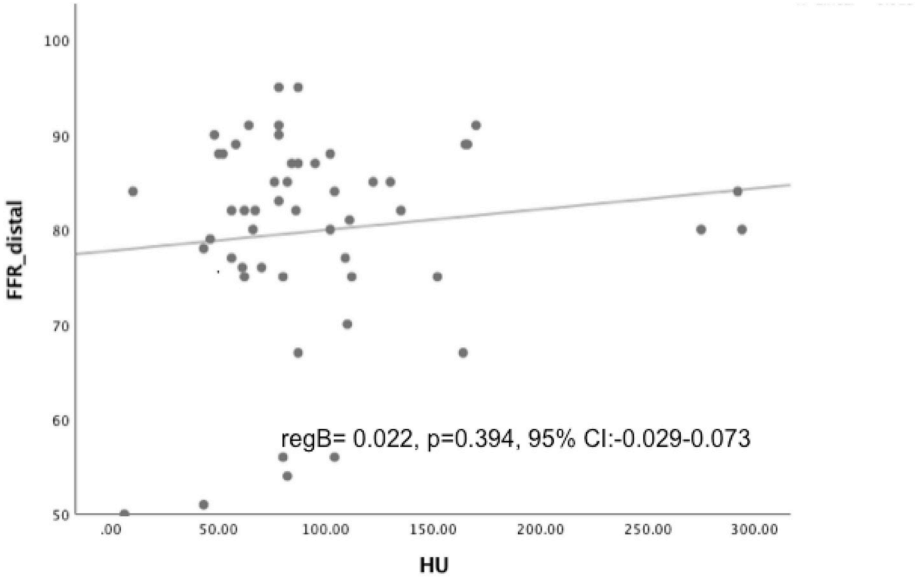

Fig. 2b. The association of low attenuation plaque density (HU) with lower distal FFR_{CT} (n = 52).

Table 3b
Low attenuation plaque (n = 52): Napkin Ring Sign and spotty calcification: distal and lesion FFR_{CT}.

	Napkin Ring Sign N = 15	No N = 37	
lesion FFR_{CT}	0.87 ± 0.08	0.82 ± 0.12	p = 0.093
distal FFR_{CT}	0.81 ± 0.08	0.76 ± 0.13	p = 0.284
	Spotty calcification N = 30	No N = 22	
lesion FFR_{CT}	0.86 ± 0.11	0.86 ± 0.08	p = 0.670
distal FFR_{CT}	0.80 ± 0.10	0.79 ± 0.11	p = 0.469

Abb. FFR = fractional flow reserve; Ca = calcified; *Mann Whitney *U* test, **Fisher exact, ***Chi-Square. Means ± SD, n = counts (%).

per group).

Quantitative CTA lumen size and % stenosis results (MLA; MLD; % area and % diameterstenosis) were tested for differences among lesions groups (HRP vs Ca) with ANOVA and post-hoc independent *t*-test.

Table 4
Quantitative CTA stenosis parameters.

	High risk plaque N = 40	Calcified N = 40	*t*-test
MLA mm^2	5.57 ± 4.1	6.4 ± 4.3	p = 0.430
MLD mm	2.04 ± 1.1	2.27 ± 1.1	p = 0.392
% area stenosis	42.3 ± 20.8	34.9 ± 14.2	p = 0.086
% diameter stenosis	25.1 ± 14.3	20.0 ± 8.7	p = 0.077

Abb. MLA = minimal lumen area, MLD = minimal lumen diameter.

Correlation coefficients (Spearman for non-normally distributed, and Pearson, for normal distributed data) between CTA data (HU- of LAP and all lesions, PR, SIS, CCS, G-score) and FFR_{CT} were determined.

Univariate linear regression analysis was performed to assess[1] the association between the plaque HU (for both LAP and all lesions) with lesion-based and distal FFR_{CT}[2]; the correlation of remodelling index (RI) with distal FFR_{CT}[3] the correlation of plaque burden scores (G-score, SIS and Calcium score) with distal FFR_{CT}.

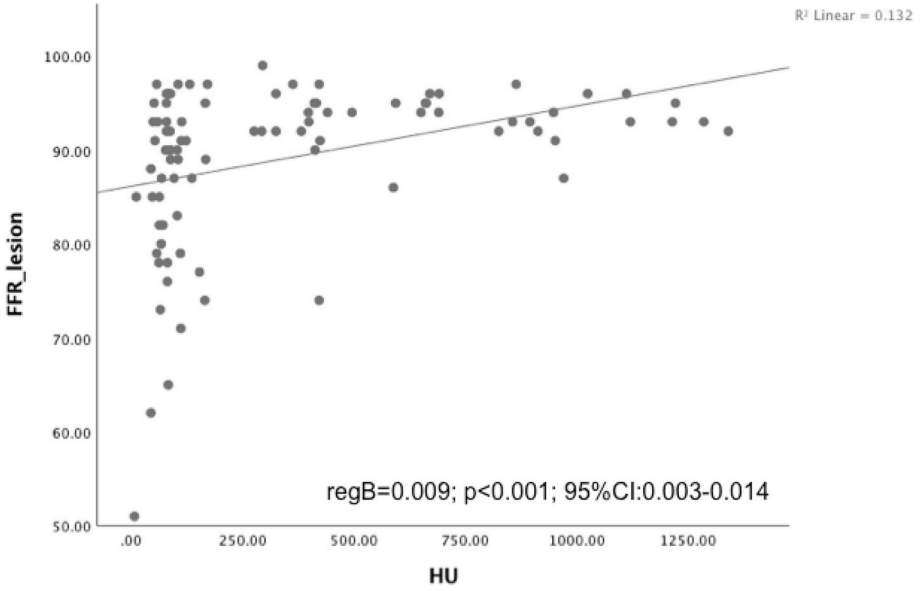

Fig. 2c. The association of increasing plaque density with higher lesion FFR_{CT} (all lesions, n = 89, calcified and low-attenuation lesions).

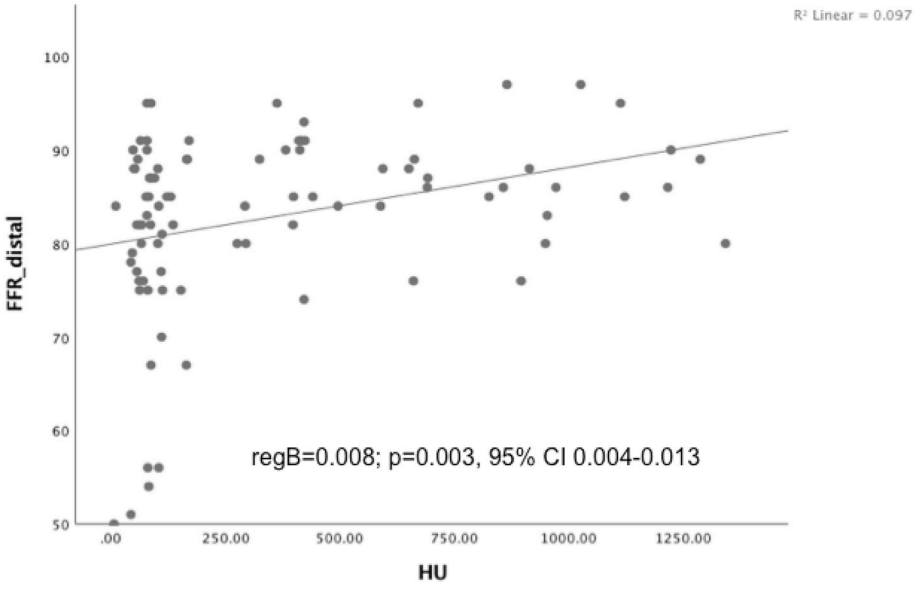

Fig. 2d. The association of increasing plaque density with higher distal FFR_{CT} (all lesions, n = 89).

Statistical analysis was performed using IBM SSPS™ software (*V25.0, IBM Corporation, Armonk, NY; USA)* . A *p*-value of less than 0.05 was considered as significant.

3. Results

Out of 106 patients, 89 lesions with optimal image quality were included (40 HRP, 40 Ca, matched for stenosis %, and 9 non-calcified). Lesions with limited image quality (e.g. due to artifacts such as motion) that could not be postprocessed by FFR analysis were excluded. Table 1 shows study cohort profile. Table 2 shows lesion characteristics (CADRADS stenosis severity, plaque composition type 1–4; and AHA segments). The majority of lesions were CADRADS 2 or 1 (**89.9%)**, and the minority 3 (10.1%).

High-risk plaque and calcified plaque compared to FFR_{CT}: Lesion and distal FFR_{CT} were significantly lower in high-risk plaque as compared to calcified ($p < 0.001$ and $p = 0.002$) (Table 3a).

Prevalence of lesion-based and distal ischemia ($FFR_{CT} < 0.8$) was higher in high-risk plaque as compared to calcified (25% vs 2.5%, $p = 0.007$ and 40% vs 17.5%; $p = 0.048$), resp.

Low attenuation plaque density (HU) compared to FFR_{CT} (n = 52): A moderate correlation between decreasing HU and lesion FFR_{CT} was found ($R = 0.312$; $p = 0.024$). Linear regression predicted only lesion based FFR_{CT} (Fig. 2a) but not distal FFR_{CT} ($R = 0.121$, $p = 0.394$) while a minor trend was present (Fig. 2b).

There was no difference in lesion-based and distal FFR_{CT} in patients with the Napkin-Ring-Sign (n = 15) and without, though for lesion FFR_{CT}, a trend ($p = 0.093$) was found for NRS, but not for SC. (Table 3b). There was no difference in the prevalence of ischemia ($FFR_{CT} < 0.8$).

QCTA stenosis % and lumen size (MLA; MLD, % area and % diameter stenosis) were not different between the groups ($p = 0.430$; $p = 0.392$; $p = 0.086$; $p = 0.077$) (Table 4).

Plaque density (HU) plotted against FFR_{CT} (all lesions, n = 89) on linear regression (n = 89) enhanced the correlation ($R = 0.363$, $p < 0.001$) for both lesion-based (Fig. 2c) and distal FFR_{CT}.

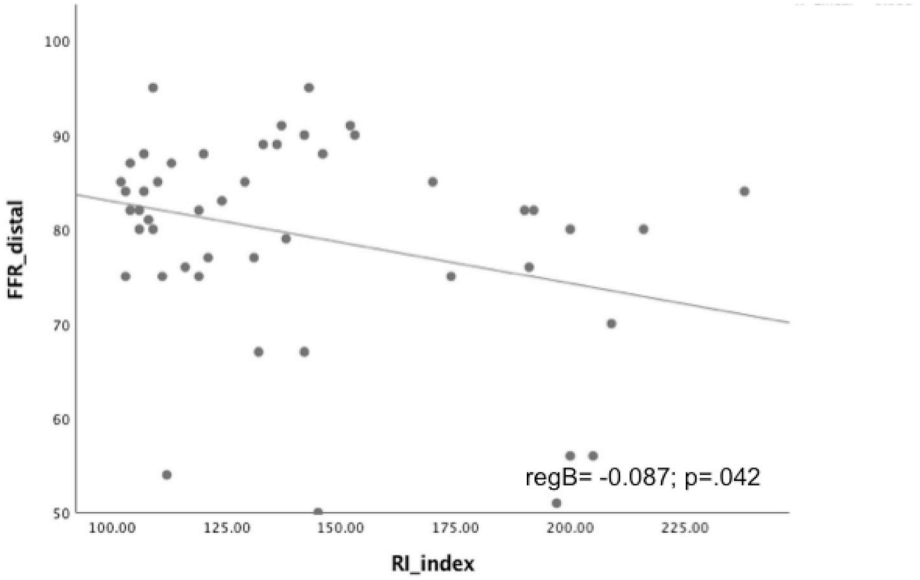

Fig. 3. The remodelling index (RI) was inversely correlated with distal FFR_{CT}.

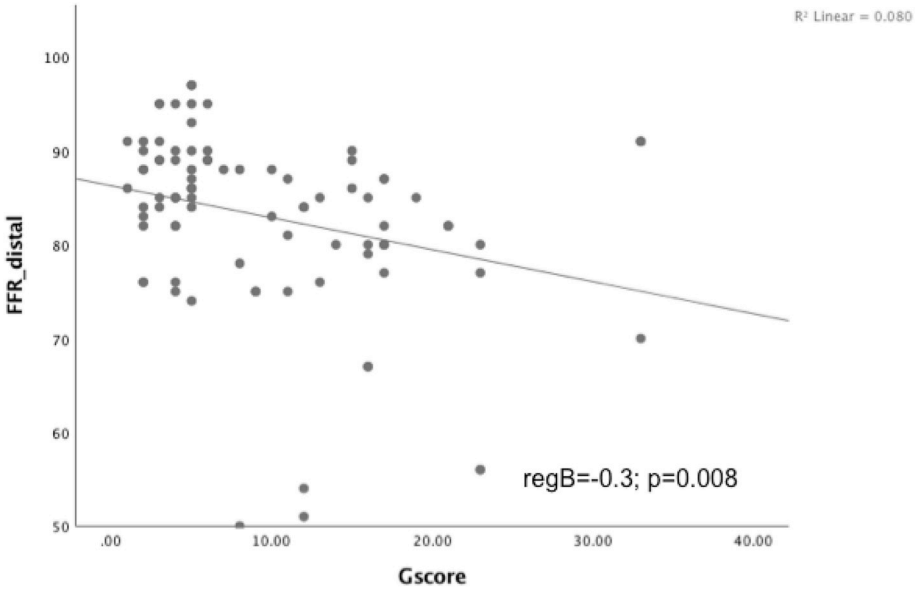

Fig. 4. Increasing non-calcified plaque burden (G-score) was correlated with lower distal FFR_{CT}.

Table 5
Plaque burden for prediction of distal FFR_{CT}.

	Distal FFR_{CT}	median
G-score	r = 0.327, p = 0.002*	7.97 (range, 1–33)
SIS	r = −0.093; p = 0.389*	4.6 (range, 0–13)
Calcium Score	r = 0.084, p = 0.438 *	101.9 AU (range, 0–683.5)

Abb. G-score = noncalcified plaque burden score (Sum of Type 1–4), SIS = segment involvement score, AU = Agatston Units, AU, r = correlation coefficient (Spearman), R = linear regression; *Spearman; **linear regression.

(R = 0.312; p = 0.003) (Fig. 2d) as compared to low attenuation plaque alone. Mean CT-density of all lesions (n = 89) was 353 HU (range, 6–1341).

An increasing positive remodelling index was also correlated with lower FFR_{CT} distal (p = 0.042, 95%CI -0.171 to −0.004) (Fig. 3).

Plaque burden and its correlation with distal ischemia. G-score and distal FFR_{CT} were correlated (Spearman r = 0.32, p = 0.002*) on linear regression (R = −0.3; p = 0.008; 95%CI -0.589–0.092) (Fig. 4); but not the SIS (r = −0.093; p = 0.389) and the coronary calcium score (r = 0.084, p = 0.438 *) (Table 5).

Fig. 5 illustrates cases examples. High risk plaque, and an increasing non-calcified plaque burden were associated with lower FFR_{CT}.

4. Discussion

First, our study showed that high-risk plaque (HRP) in non-obstructive lesions predict ischemia (**INOCA = ischemia in non obstructive coronary artery stenosis)**, but not calcified.

Our study is the first larger selected cohort of non-obstructive lesions utilizing both CTA and FFR_{CT}. Previous studies included mainly obstructive vessels (prevalence ≈80%),[18,27] or enrolled low sample sizes,[24,25] but observed a similar trend.[24–27]

The 5 novelities of our study comprise:

- The inclusion of non-obstructive lesions only, with the majority

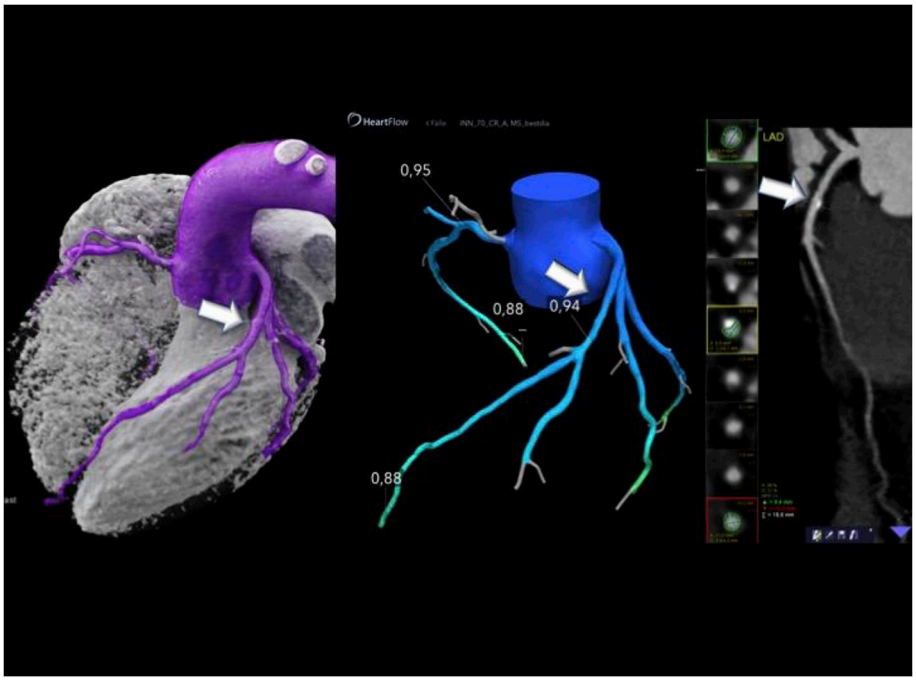

Fig. 5. a51 YOM with nonspecific symptoms (ECG:tachyarrythmia), 1 risk factor. LAD: calcified **T1 plaque** (593 HU), 21% stenosis. Distal high FFR_{CT} = 0.88 and high lesion FFR_{CT}0.94, no ischemia. Low G-score = 2 and SIS = 2.

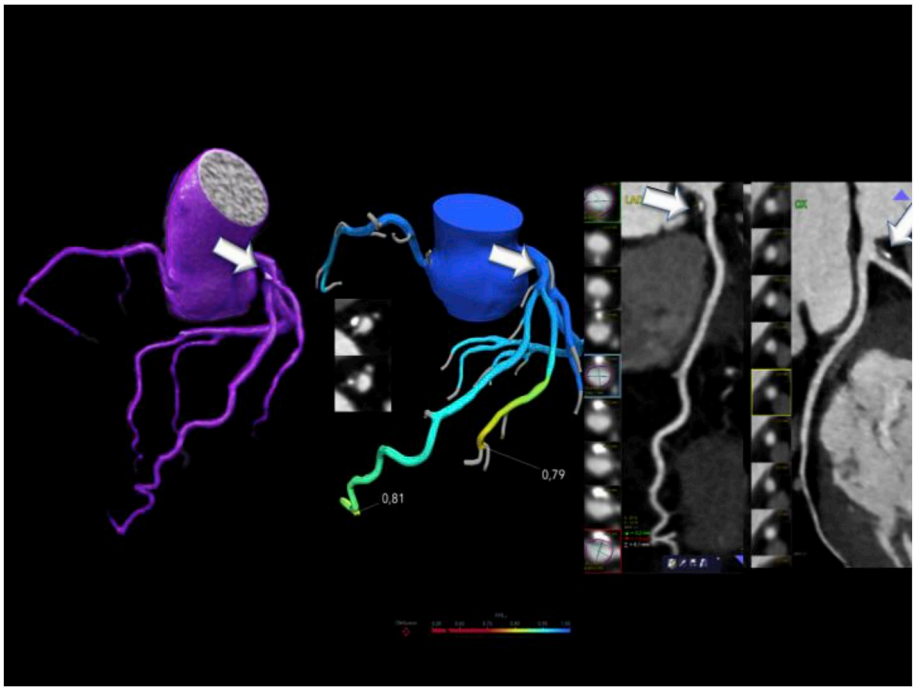

Fig. 5b. 65 YOM with atypical CP.1 risk factor. LAD: mixed plaque **TYPE 2** (dominant calcified), 14% stenosis, distal borderline FFR_{CT} = 0.81 (LAD) and 0.79 (DG1), no clear ischemia. Low G-score 3 and SIS 1. Calcium Score 54.7AU.

beeing CADRADS 1 and 2 (89.9%) and matched quantitative luminal dimensions in high-risk plaque and calcified lesions.
- CT density (HU) of calcified plaque
- The inauguration of new easy-to-implement non-calcified plaque burden score **(G-score)** (Fig. 1)

Our results **may** explain atypical chest pain related to ischemia in patients with non-obstructive lesion on coronary CTA **related to increasing non-calcified plaque component and high-risk plaque features**. These patients may also rather benefit from targeted medication regimens. Coronary atherosclerosis is a known trigger for endothelial dysfunction over reduced NO- bioavailability.[18,29] Lipid-necrotic core plaque may be causative, as indicated by IVUS studies.[30] Our results also explain, why some patients do not, or not as well respond to nitrates or other medication. Our findings are in line with another study[27] in which a low attenuation plaque component > 30 mm^2 [27] -and FFR_{CT} adds diagnostic yield over stenosis% assessment stand alone, for prediction of ischemia. The prevalence of nonobstructive

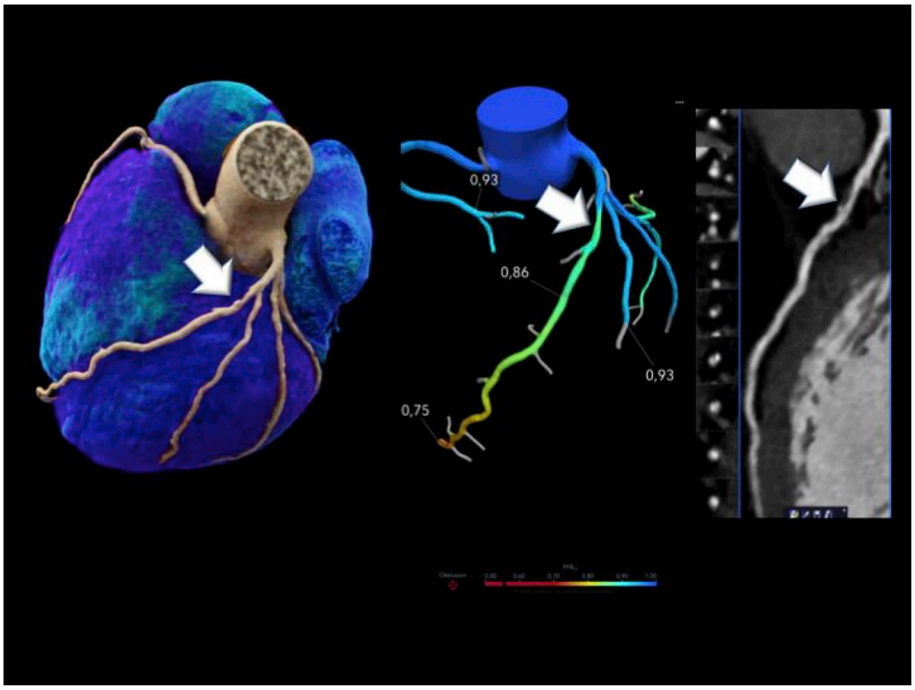

Fig. 5c. 45 YOM with atypical CP, 4 risk factors (smoker 1pack/week/30y). LAD: mixed **plaque TYPE 3** (dominantly non-calcified) with **high-risk plaque criteria** (LAP 53 HU, Spotty Calcification, positive remodelling). Distal boderline ischemia FFR_{CT} = 0.75 despite only 20% diameterstenosis. High G-score 13. SIS 4. Calcium Score 1.1AU minimal.

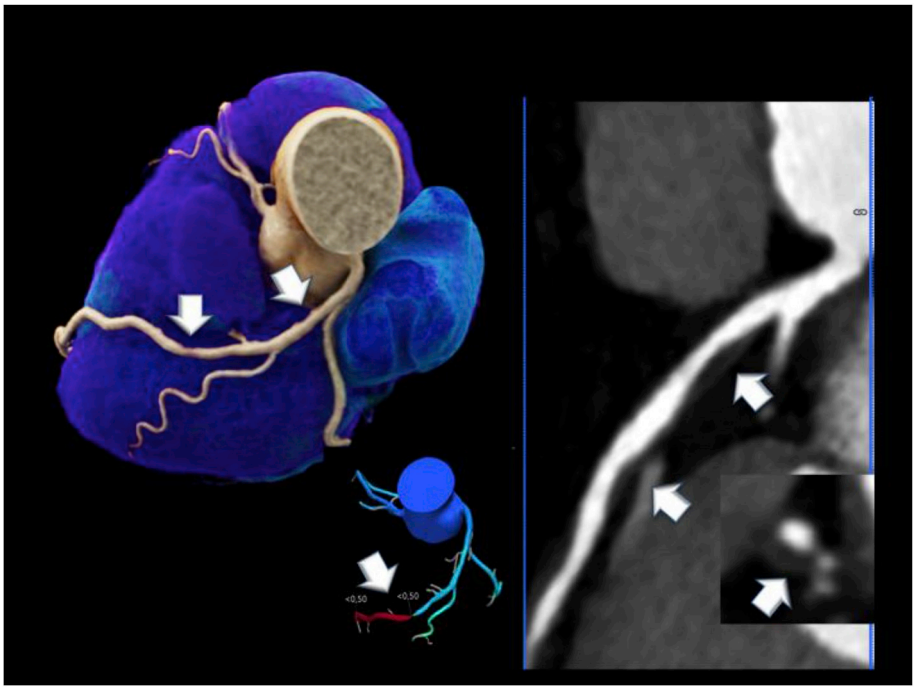

Fig. 5d. 67 YOM with atypical CP. LAD: 2 tandem non-calcified plaque (type 4) with 3 high-risk plaque criteria: low attenuation 6HU (lipid-rich core), Napkin Ring Sign, RI > 1.1, causing both lesion-based and distal ischemia (**FFR_{CT}** = 0.5). High G-score of 12. SIS 3. Calcium Score zero.

lesions though was low with 21% in this trial.[27]

Second, our data revealed that a declining plaque density (HU) was associated with lower lesion FFR_{CT}. A decreasing plaque density towards 0 HU indicates an increasing lipid-rich necrotic core. While different density cut-offs (< 30HU and 60 HU)[13,14] have been proposed for detection of lipid-rich inflammatory thin-cap fibroatheroma,[13] a significant overlap in HU is well known due to individual lesion differences[23] and radiation physics.

Noncalcified fibroatheroma by coronary CTA are known indicators for prediction of major adverse cardiac events (MACE).[16,17] A hypodense low-attenuating plaque component on CTA is visualized darker as compared to the i iodine contrast agent (200-400HU). Various thresholds (< 150 HU,[28] < 30HU[14] or < 60 HU[16] have been tested for prediction of MACE, and all were significant.[16,17]

Based on physical principles, however, it is not reliable to set a fixed cut-off for each lesion, based on the natural diversity in HU, representing the x-ray absorption value (HU) of an image voxel. The HU are influenced by a wide array of individual factors, such as artifacts and the x-ray absorption of surrounding tissue, thus, significant overlaps in HU between fibrous and lipid-rich plaque were found in comparative studies with IVUS.[23] A “fading” declining relationship in HU with a grey zone may be an even better marker for defining “high-risk”

lesions than a fixed cut-off, because not only lipid-rich plaque are causing MACE event: PROSPECT study data (using OCT) revealed that thrombotic events were even more often characterized by *superficial plaque erosion*[33] lesions with accumulated proteogylcans which had a thicker fibrous cap and less inflammatory cells, possibly exhibiting higher HU (30 HU up to 150HU) than lipid rich.

Our findings are in line with a recent subanalysis of NXT,[18] in which necrotic core volume was an independent predictor of ischemia by invasive FFR in 254 patients. In contrast to our study, the prevalence of non-obstructive lesions in the NXT trial was low with 20% but nonetheless, ischemia was found frequently.[18]

Further, the high prevalence of ischemia in non-obstructive lesions with high-risk plaque features (40% and 25% for lesion based and distal FFR_{CT}), but not in calcified, was surprisingly high in our cohort. This may also explain the dicrepany in outcomes associated with FFR-guided therapy (RIPCORD-trial).[7] The RIPCORD trial is a prospective randomized trial enrolling 200 patients with chest pain, showing that FFR_{CT} significantly impacts patient management: In 36%, CTA stenosis severity and patient managment was changed, after adding FFR_{CT}.

Third, our study shows, for the first time, a correlation of increasing plaque density, also for calcified lesions (HU) and low attuation plaque, with declining ischemia. The HU–density of a calcified nodule is highly variable, ranging from > 150HU up to > 1000HU, pending on its individual crystallization stage and compactness, and its specific chemical composition (mainly hypdroxylapatit-prestages or advanced formulas; or whitelockit).[34] Beyond, the shape and distribution of calcium in vessel walls on coronary CTA is varying, ranging from tiny spotty calcification < 3 mm over tram-track like medial calcification. Low density calcium may even appear "isoisodense" to the intraluminal contrast agent and may be difficult to visualize. The location of calcium along the coronary tree -on a tortous, stretched, or side branching site-, as well impacts the crystallization stage and its compactness, related to wall sheer stress.[34] Our results also explain the wide spectrum of discrepancy in ischemia and % stenosis: Even severe stenosis > 70% may not necessarily cause ischemia: In the FAME-trial, 20% of lesions with severe 70–90% stenosis and 35% with intermediate 50–70% stenosis were non-ischemic.[30]

Beyond, our study confirmed the correlation of increasing positive remodelling (Fig. 3), with distal low FFR_{CT}. However, there was not correlation found for spotty calcification, in line with another study.[31] Further, we observed a minor trend towards an association between the Napkin Ring Sing (synomyn "Half- Moon" Sign) and lower lesion-based FFR_{CT}.

Forth, we describe a novel plaque type score based on 4 types; per coronary-AHA-16-segment classification, the **"G-score"** (Fig. 1). The G-score is an easy visual look-up score, for estimation of mixed including non-calcified plaque burden. An increasing G-score predicts distal ischemia and may explains atypical chest pain related to ischemia. Hence this information is helpful for patient communication. Patients with increasing G-score may further benefit from specific medication such as statins or PSCK-9 inhibitors.

In line with the G-score, 2 other studies[24,25] found that % plaque volume (PV) rather than qCTA stenosis predicted ischemia (n = 18 non–obstructive)[25]; and %APV (aggregate plaque volume) in n = 58 intermediate lesions (38% obstructive -causing ischemia).[24] In a larger series,[31] a 50% increased risk of ischemia per 5% APV (n = 151; total 37% ischemic lesions) was reported. While %APV reflects an excellent predictor for MACE[32], the difficulty in translating APV quantification into practice, lies in the high rate of inaccurate outer vessel contour tracing results (up to 90%), requireing manual adjustments. Such edits are very time consuming to date, while summing up the G-score takes only about 1 min after consolidating a structured clinical coronary CTA report. Time–saving AI-assisted tools based on machine learning algorithms may hopefully solve this task in the future[35](26).

Study limitations. The prevalence of the Napkin Ring Sign was low. FFR_{CT} was determined computational based on CT data but not invasively.

5. Conclusions

- Non-obstructive high risk plaque and an increasing non-calcified plaque burden (G-score) by coronary CTA are associated with myocardial ischemia (INOCA) but not calcified, with a surprisingly high prevalence **(25% and 40% for lesion based and distal FFR_{CT}) for high risk plaque.** Especially those patients may benefit from targeted medication.
- A higher lipid-necrotic core plaque component and positive remodelling is associated with lower FFR_{CT}*; while an* **increasing fibrocalcific plaque density acts contrary.**

Authors statement

The project was supported by a research agreement with Heartflow Inc.

References

1. Douglas PS, Hoffmann U, Patel MR, et al. PROMISE Investigators.Anatomical versus functional testing for coronary artery disease. *N Engl J Med.* 2015;373(1):1291–1300.
2. Budoff MJ, Dowe D, Jollis JG, et al. Diagnostic performance of 64-multidetector row coronary computed tomographic angiography for evaluation of coronary artery stenosis in individuals without known coronary artery disease: results from the prospective multicenter ACCURACY (Assessment by Coronary Computed Tomographic Angiography of Individuals Undergoing Invasive Coronary Angiography) trial. *J Am Coll Cardiol.* 2008;52(21):1724–1732.
3. Nakazato R, Arsanjani R, Achenbach S, et al. Age-related risk of major adverse cardiac event risk and coronary artery disease extent and severity by coronary CT angiography: results from 15 187 patients from the International Multisite CONFIRM Study. *Eur Heart J Cardiovasc Imaging.* 2014;15(5):586–594.
4. Leipsic J, Yang TH, Thompson A, et al. CT angiography (CTA) and diagnostic performance of noninvasive fractional flow reserve: results from the Determination of Fractional Flow Reserve by Anatomic CTA (DeFACTO) study. *AJR Am J Roentgenol.* 2014;202(5) 989-9.
5. Nørgaard BL, Leipsic J, Gaur S, et al. NXT Trial Study Group.Diagnostic performance of noninvasive fractional flow reserve derived from coronary computed tomography angiography in suspected coronary artery disease: the NXT trial (Analysis of Coronary Blood Flow Using CTAngiography: next Steps). *J Am Coll Cardiol.* 2014;63(12):1145–1155.
6. Hlatky MA, De Bruyne B, Pontone G, et al. PLATFORM investigators. Quality-of-Life and economic outcomes of assessing fractional flow reserve with computed tomography angiography: PLATFORM. *J Am Coll Cardiol.* 2015;66(21):2315–2323.
7. Curzen NP, Nolan J, Zaman AG, Nørgaard BL, Rajani R. Does the routine availability of CT-derived FFR influence management of patients with stable chest pain compared to CT angiography alone?: the FFRCT RIPCORD study. *JACC Cardiovasc Imaging.* 2016;9(10):1188–1194.
8. Tesche C, De Cecco CN, Albrecht MH, et al. Coronary CT angiography-derived fractional flow reserve. *Radiology.* 2017;285(1):17–33.
9. Pijls NH, van Schaardenburgh P, Manoharan G. Percutaneous coronary intervention of functionally nonsignificant stenosis: 5-year follow-up of the DEFER Study. *J Am Coll Cardiol.* 2007;49(21):2105–2111.
10. De Bruyne B, Fearon WF, Pijls NH, et al. FAME 2 Trial Investigators.Fractional flow reserve-guided PCI for stable coronary artery disease. *N Engl J Med.* 2014;371(13):1208–1217.
11. Park HB, Lee BK, Shin S, et al. Clinical feasibility of 3D automated coronary atherosclerotic plaque quantification algorithm on coronary computed tomography angiography: comparison with intravascular ultrasound. *Eur Radiol.* 2015;25(10):3073–3083.
12. Maurovich-Horvat P, Schlett CL, Alkahdi H, et al. The napkin-ring sign indicates advanced atherosclerotic lesions in coronary CT angiography. *JACC Cardiovasc Imaging.* 2012;5(12):1243–1245.
13. Nakazato R, Otake H, Konishi A, et al. Atherosclerotic plaque characterization by CT angiography for identification of high-risk coronary artery lesions: a comparison to optical coherence tomography. *Eur Heart J Cardiovasc Imaging.* 2015;16(4):373–379.
14. Marwan M, Taher MA, El Meniawy K, et al. In-vivo CT detection of lipid-rich coronary artery atherosclerotic plaques using quantitative histogram analysis: a head to head comparison with IVUS. *Atherosclerosis.* 2011;215(1):110–115.
15. Schlett CL, Maurovich-Horvat P, Ferencik M, et al. Histogram analysis of lipid-core plaques in coronary computed tomographic angiography: ex vivo validation against histology. *Invest Radiol.* 2013;48(9):646–653.
16. Feuchtner G, Kerber J, Burghard P, et al. The high-risk criteria low-attenuation plaque < 60 HU and the napkin-ring sign are the most powerful predictors of MACE: a long-term follow-up study. *Eur Heart J Cardiovasc Imaging.* 2017;18(7):772–779.
17. Thomsen C, Abdulla J. Characteristics of high-risk coronary plaques identified by computed tomographic angiographyand associated prognosis: a systematic review and meta-analysis. *Eur Heart J Cardiovasc Imaging.* 2016;17(2):120–129.

18. Ahmadi A, Leipsic J, Øvrehus KA, et al. Lesion-specific and vessel-related determinants of fractional flow reserve beyond coronary artery stenosis. *JACC Cardiovasc Imaging.* 2018;11(4):521–530.
19. Genders TS, Steyerberg EW, Alkadhi H, et al. A clinical prediction rule for the diagnosis of coronary artery disease: validation, updating, and extension. *Eur Heart J.* 2011;32(11):1316–1330.
20. Cury RC, Abbara S, Achenbach S, et al. Leipsic JA CAD-RADS(TM) coronary artery disease - reporting and data system. An expert consensus document of the society of cardiovascular computed tomography (SCCT), the American college of radiology (ACR) and the north American society for cardiovascular imaging (NASCI). Endorsed by the American college of Cardiology. *J Cardiovasc Comput Tomogr.* 2016;10(4):269–281.
21. Austen WG, Edwards JE, Frye RL, et al. A reporting system on patients evaluated for coronary artery disease. Report of the ad hoc committee for grading of coronary artery disease, council on cardiovascular surgery, American heart association. *Circulation.* 1975;51(4 Suppl):5–40.
22. Feuchtner G, Postel T, Weidinger F, et al. Is there a relation between non-calcifying coronary plaques and acute coronary syndromes? A retrospective study using multislice computed tomography. *Cardiology.* 2008;110(4):241–248.
23. Leber AW, Knez A, Becker A, et al. Accuracy of multidetector spiral computed tomography in identifying and differentiating the composition of coronary atherosclerotic plaques: a comparative study with intracoronary ultrasound. *J Am Coll Cardiol.* 2004;43(7):1241–1247.
24. Nakazato R, Shalev A, Doh JH, et al. Aggregate plaque volume by coronary computed tomography angiography is superior and incremental to luminal narrowing for diagnosis of ischemic lesions of intermediate stenosis severity. *J Am Coll Cardiol.* 2013;62(5):460–467.
25. Kato N, Kishi S, Arbab-Zadeh A, et al. Relative atherosclerotic plaque volume by CT coronary angiography trumps conventional stenosis assessment for identifying flow-limiting lesions. *Int J Cardiovasc Imag.* 2017;33(11):1847–1855.
26. Rizvi A, Hartaigh BÓ, Danad I, et al. Diffuse coronary artery disease among other atherosclerotic plaque characteristics by coronarycomputed tomography angiography for predicting coronary vessel-specific ischemia by fractional flow reserve. *Atherosclerosis.* 2017;258:145–151.
27. Gaur S, Øvrehus KA, Dey D, et al. Coronary plaque quantification and fractional flow reserve by coronary computed tomography angiography identify ischaemia-causing lesions. *Eur Heart J.* 2016;37(15):1220–1227.
28. Ferencik M, Mayrhofer T, Puchner SB, et al. Computed tomography-based high-risk coronary plaque score to predict acute coronary syndrome among patients with acute chest pain - results from the ROMICAT II trial. *J Cardiovasc Comput Tomogr.* 2015;9(6):538–545.
29. Ahmadi A, Kini A, Narula J. Discordance between ischemia and stenosis, or PINSS and NIPSS: are we ready for newvocabulary? *JACC Cardiovasc Imaging.* 2015;8(1):111–114.
30. Park SJ, Kang SJ, Ahn JM, et al. Visual-functional mismatch between coronary angiography and fractional flow reserve. *J Am Coll Cardiol Intv.* 2012;5(10):1029–1036.
31. Park HB, Heo R, ó Hartaigh B. Atherosclerotic plaque characteristics by CT angiography identify coronary lesions that cause ischemia: a direct comparison to fractional flow reserve. *J Am Coll Cardiol Img.* 2015;8(1):1–10.
32. Hell MM, Motwani M, Otaki Y, et al. Quantitative global plaque characteristics from coronary computed tomography angiography for the prediction of future cardiac mortality during long-term follow-up. *Eur Heart J Cardiovasc Imaging.* 2017;18(12):1331–1339.
33. Libby P, Pasterkamp G. A requiem for the vulnerable plaque? *Eur Heart J.* 2015;36(43):2984–2987.
34. You AYF, Bergholt MS, St-Pierre JP, et al. Raman spectroscopy imaging reveals interplay between atherosclerosis and medialcalcification in the human aorta. *Sci Adv.* 2017;3(12):e1701156.
35. Singh G, Al'Aref SJ, Van Assen M, et al. Machine learning in cardiac CT: basic concepts and contemporary data. *J Cardiovasc Comput Tomogr.* 2018;pS1934–5925(18)30084-4.